DALTON

Spectroscopic, magnetic and structural studies on the mixed-valence cuboidal clusters $[Mo_4E_4(edta)_2]^{3-}$ (E = S or Se; H_4edta = ethylenediaminetetra-acetic acid) and $[Mo_4S_4(H_2O)_{12}]^{5+}$†

William McFarlane,[a] Mohamed Nasreldin,[a] David M. Saysell,[a] Zhi-Shen Jia,[a] William Clegg,[a] Mark R. J. Elsegood,[a] Keith S. Murray,[b] Boujemaa Moubaraki[b] and A. Geoffrey Sykes,*[,a]

[a] *Department of Chemistry, University of Newcastle, Newcastle upon Tyne NE1 7RU, UK*
[b] *Department of Chemistry, Monash University, Clayton, Victoria, Australia*

The ^{77}Se NMR spectrum of the mixed-valence cluster $[Mo_4Se_4(edta)_2]^{3-}$ (H_4edta = ethylenediamine-*N,N,N′,N′*-tetraacetic acid) was recorded and appears to be consistent with the presence in solution of a valence-trapped species $Mo^{III}{}_3Mo^{IV}$ with a lifetime in excess of 10^{-5} s. However this was not supported by ^{95}Mo and ^{77}Se NMR studies on other $[Mo_4Se_4(edta)_2]^{n-}$ (n = 2 or 4) clusters. Overall it appears that multiple NMR signals arise from the presence in solution of species which differ slightly from the above formulae in the extent of co-ordination of H_2O and edta. The studies do not preclude the possibility of valence-trapped species with lifetimes shorter than 10^{-6} s. A model in which intervalence electron exchange within the core clusters $Mo_4E_4{}^{5+}$ (E = S or Se) is slower than formation/decay ($\approx 10^9$ s^{-1}) of ion-pair precursors is proposed to account for the biphasic kinetic behaviour previously observed for substitution of H_2O on $[Mo_4S_4(H_2O)_{12}]^{5+}$. The crystal structure of a hydrated sodium salt of $[Mo_4Se_4(edta)_2]^{3-}$ has been determined, and is compared to that previously obtained for $[Mo_4S_4(edta)_2]^{3-}$. Other techniques explored include magnetic moment measurements on a solid sample of $[Mo_4S_4(H_2O)_{12}][pts]_5\cdot 14H_2O$ (pts = toluene-*p*-sulfonate) which show a Curie-like behaviour ($\chi = C/T$) for an $S = \frac{1}{2}$ ground state, with a corresponding magnetic moment independent of temperature over the range 300–4.2 K. Metal–ligand stretching frequencies from Fourier-transform IR studies on the chloride salt of the same 5+ cluster have also been obtained.

The present studies were prompted by equilibration kinetic studies on 1:1 thiocyanate substitution reactions, NCS^- for H_2O, at the molybdenum of cuboidal clusters $[Mo_4S_4(H_2O)_{12}]^{4+}$ and $[Mo_4S_4(H_2O)_{12}]^{5+}$ in aqueous acidic solutions, I = 2.00 M ($LiClO_4$).[1] Both the NCS^- reactions were found to be slow with reaction times (as illustrated) of 3–4 and 50 h respectively.‡ In the case of the 4+ $Mo^{III}{}_4$ cube the forward rate constant k_f is 1.95 M^{-1} s^{-1}, and a statistical factor of 4 was identified corresponding to the number of equivalent molybdenum centres.[2,3]§ With the 5+ cube biphasic kinetics is observed, and two $[NCS^-]$-dependent reaction steps are clearly apparent. For the first a statistical factor of 3 applies, and the rate constant k_{1f} = 0.116 M^{-1} s^{-1} is assigned to substitution at each of three molybdenum(III) centres. For the second there is no statistical factor, and k_{2f} = 0.0166 M^{-1} s^{-1} was assigned to substitution at a single Mo^{IV}. Such studies on $[Mo_4S_4(H_2O)_{12}]^{5+}$ provide evidence therefore for an electron distribution approximating to $Mo^{III}{}_3Mo^{IV}$. The aim of the present work is to elaborate further on the evidence for a localised $Mo^{III}{}_3Mo^{IV}$ structure using different techniques. Of these NMR spectroscopy was thought to have the most potential and is at the forefront of the studies described.

In addition to using ^{95}Mo we decided to study the cuboidal cluster Mo_4Se_4 by ^{77}Se NMR spectroscopy (both isotopes at natural abundance). However the latter cube is not sufficiently stable as $[Mo_4Se_4(H_2O)_{12}]^{5+}$ for the duration of the NMR experiments envisaged,[4] and we therefore used the more stable $[Mo_4Se_4(edta)_2]^{3-}$ analogue (H_4edta = ethylenediamine-*N,N,N′,N′*-tetraacetic acid). Depending upon the chemical shift separations in the ^{77}Se and ^{95}Mo spectra, it should in principle be possible to detect species with lifetimes as short as 10^{-4}–10^{-6} s. As part of the characterisation the crystal structure of a hydrated sodium salt of $[Mo_4Se_4(edta)_2]^{3-}$ was determined, thus completing the series alongside $[Mo_4S_4(edta)_2]^{3-}$, $[Mo_4S_4(H_2O)_{12}]^{5+}$ and $[Mo_4Se_4(H_2O)_{12}]^{5+}$.[5,6] We also extend previous magnetic moment measurements on samples of $[Mo_4S_4(edta)_2]^{n-}$, n = 2–4,[7] to include studies on $[Mo_4S_4(H_2O)_{12}]^{5+}$ and report infrared studies on the latter.

Experimental

Preparations

$[Mo_4Se_4(edta)_2]^{3-}$. The di-μ-selenido-dimolybdate(V) complex $[Mo_2O_2(\mu\text{-}Se)_2(edta)]^{2-}$ was first prepared by 1:1 addition of disodium dihydrogenethylenediaminetetraacetate to a solution of $[Mo_2O_2(\mu\text{-}Se)_2(H_2O)_6]^{2+}$,[4] peak positions λ/nm 247, 303, 330 (sh) and 419, and adjusting the pH to ≈6 using $NaHCO_3$ (solid). The pale orange solid was recrystallised from water to give $Na_2[Mo_2(\mu\text{-}Se_2)_2(edta)]\cdot 2H_2O$. In order to bring about dimerisation of the Mo_2Se_2 ring and generate cuboidal Mo_4Se_4, the $Mo^V{}_2$ complex (2 g) in 0.03 M HCl (200 cm^3) was reduced on addition to sodium tetrahydroborate, $NaBH_4$ (1 g), under a dinitrogen atmosphere. The resultant solution was left air-free overnight at ≈4 °C, then heated in air at 90 °C for 20 h. It changed gradually from an initial

---

† *Non-SI units employed:* M = mol dm^{-3}, $\mu_B \approx 9.27 \times 10^{-24}$ J T^{-1}, emu = SI × $10^{-6}/4\pi$.

‡ All the sulfur atoms in the cubes are μ_3-bridging and do not appear to labilise ligands on the molybdenum centres. A different situation has been shown to apply in the trinuclear complex $[Mo_3S_4(H_2O)_9]^{4+}$ which has one μ_3-S and three electron-rich μ-S atoms in the core. The latter produce a labilising effect on the H_2O in the *trans* positions (six in all), whereas the other three H_2O ligands *trans* to the μ_3-S are inert.[2,3]

§ A statistical factor is defined as the ratio of rate constants for complex-formation with the cube in > 10-fold excess to that with NCS^- in > 10-fold excess. Whereas the reaction with the cube in excess is restricted to substitution of at one of a number of equivalent molybedenum centres, with NCS^- in excess reaction occurs concurrently at that number of centres.

dark brown to dark green. After filtration the products were concentrated using a rotary evaporator, and subjected to Sephadex G-10 (25 × 1.5 cm diameter) column chromatography (Sigma Chemicals). Yield 20%. Final purification was on a QAE-Sephadex anion-exchange column (25 × 1.5 cm diameter) equilibrated with 0.10 M NaCl. Sufficient NaCl was added to the green solution to give a 0.10 M NaCl solution prior to loading. After washing with 0.10 M NaCl (or $LiClO_4$), $[Mo_4Se_4(edta)_2]^{3-}$ was eluted with 0.25 M NaCl (or $LiClO_4$). The UV/VIS/NIR spectrum of $[Mo_4Se_4(edta)_2]^{3-}$ in 0.50 M $LiClO_4$ has peaks λ/nm (ε/M^{-1} cm^{-1} per cube) at 659 (515) and 1200 (155), see Fig. 1. Slow vapour diffusion of acetone into a solution of $[Mo_4Se_4(edta)_2]^{3-}$ in 0.25 M NaCl gave green crystals of the hydrated sodium salt of $[Mo_4Se_4(edta)_2]^{3-}$. These were dissolved in aqueous $LiClO_4$ to give solutions of the required concentration for NMR studies. Over extended periods the solutions were stored under N_2 at 4 °C.

$[Mo_4Se_4(edta)_2]^{2-}$. A solution containing $[Mo_4Se_4(edta)_2]^{3-}$ (10 cm^3, 1–10 mM) in 1 M $LiClO_4$ was oxidised under an N_2 atmosphere at a carbon-cloth electrode (RGV 1000, Le Carbonne, Brighton) using a constant potential of +0.50 V (*vs.* standard calomel electrode, SCE).[8] An all-glass electrolytic cell (5.5 cm high, 3 cm diameter), having an ≈0.8 cm diameter finger closed at the bottom with a No. 3 sinter glass frit as anode compartment was used. A platinum-foil anode and standard calomel reference electrode were used. The carbon cloth of the cathode was wrapped around a glass rod and tied in position with Teflon tape. Electrical contact was made by attaching a carbon rod to the upper end of the glass rod using epoxide resin. The carbon cloth covered both these sections and fitted tightly into the 0.8 cm diameter entry to the cell. Oxidation was complete in ≈2 h, and the brown solution of $[Mo_4Se_4(edta)_2]^{2-}$ was syphoned into a degassed vessel. The UV/VIS/NIR spectrum gave λ/nm (ε/M^{-1} cm^{-1} per cube) 568 (719) and 942 (359), Fig. 1. On standing at room temperature under air, red Se was deposited within 2 days. Under N_2 no similar decay process was observed.

$[Mo_4Se_4(edta)_2]^{4-}$. Crystals of the hydrated sodium salt of $[Mo_4Se_4(edta)_2]^{3-}$ (0.1 g, 0.07 mmol) were dissolved in water–D_2O (1:1, 3 cm^3), and deoxygenated using an N_2 stream. The solution was transferred to an NMR tube containing sodium dithionite (0.1 g, 0.6 mmol) (Fluka, >97%) under an N_2 atmosphere, changing immediately from green to the orange-red of $[Mo_4Se_4(edta)_2]^{4-}$, which was confirmed by the UV/VIS spectrum, peak at 415 nm (ε = 1393 M^{-1} cm^{-1} per cube), Fig. 1.

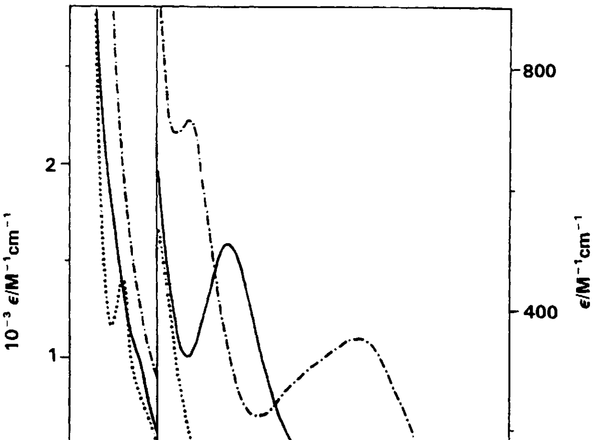

Fig. 1 The UV/VIS/NIR spectra for the series of complexes $[Mo_4Se_4(edta)_2]^{3-}$ (——), $[Mo_4Se_4(edta)_2]^{2-}$ (- • -) and $[Mo_4Se_4(edta)_2]^{4-}$ (. . .) in water

Other cuboidal complexes. Crystalline samples of $[Mo_4S_4(H_2O)_{12}][pts]_5\cdot14H_2O$ (pts = toluene-*p*-sulfonate) and solutions of $[Mo_4S_4(H_2O)_{12}]^{4+}$ (17 mM) in 2.0 M $HClO_4$ and $[Mo_4S_4(edta)_2]^{3-}$ (16 mM) in 1.0 M $LiClO_4$ were prepared as previously described.[6,8] For infrared studies solid samples of $[Mo_4S_4(H_2O)_{12}]Cl_5$ and $[Mo_3S_4(H_2O)_9]Cl_4$ were obtained by evaporating to dryness on a vacuum line at room temperature solutions eluted with 2.0 M HCl from Dowex 50W-X2 cation-exchange columns. Spectra of KBr discs were recorded on a Nicolet 20PC FTIR instrument.

X-Ray crystallography

Crystal data. $Na_{2.5}H_{0.5}[C_{20}H_{24}Mo_4N_4O_{16}Se_4]\cdot10H_2O$, $M = 1514.2$, monoclinic, space group $P2_1/c$, $a = 15.635(3)$, $b = 12.196(2)$, $c = 24.287(5)$ Å, $\beta = 97.60(3)°$, $U = 4590(2)$ Å^3, $Z = 4$, $D_c = 2.190$ g cm^{-3}, $\mu = 4.35$ mm^{-1} (Mo-Kα, $\lambda = 0.710\ 73$ Å), $F(000) = 2928$, $T = 160$ K.

Measurements were made on a Stoe-Siemens diffractometer with a Cryostream cooler,[9] from a crystal of size 0.55 × 0.16 × 0.10 mm. Cell parameters were refined from 2θ values (22–25°) of 34 reflections measured at ±ω to minimise systematic errors. Intensities were measured by ω–θ scans and on-line profile fitting;[10] $2\theta_{max} = 45°$ with a complete unique quadrant of data (*h* −16 to 16, *k* 0–13, *l* 0–26) and some Friedel opposites. Corrections were made for absorption (semiempirically from ψ scans, transmission 0.519–0.907),[11] and for an observed 1% decay in five periodically monitored standard reflections.

The structure was solved by direct methods and refined[11] on F^2 with a weighting scheme $w^{-1} = \sigma^2(F_o) + (0.062P)^2 + (133.988P)$, where $P = (2F_c^2 + F_o^2)/3$. Anisotropic displacement parameters were refined for all non-hydrogen atoms, except for six partially occupied water-molecule oxygen atoms, which were refined isotropically and with a total combined occupancy of 2. Isotropic hydrogen atoms in the anion were included with riding-model constraints and $U(H) = 1.5U_{eq}(C)$, but no water hydrogen atoms were located. The overall cation charge of +2.5, resulting from sodium ions on two general positions and an inversion centre, requires an additional $0.5H^+$ for charge balance, with the extra proton charge potentially disordered over various sites. Final $R' = \{\Sigma[w(F_o^2 - F_c^2)^2]/\Sigma[w(F_o^2)^2]\}^{\frac{1}{2}} = 0.1766$ for all 5959 unique reflections (from a total of 6782 measured data, $R_{int} = 0.0598$), conventional R [on F values of 4620 reflections with $F_o^2 > 2\sigma(F_o^2)$] = 0.0534, goodness of fit = 1.099 on F^2 for 559 refined parameters. The largest difference electron-density peaks were 1.86 e Å^{-3}, close to heavy atoms, with no holes deeper than −0.86 e Å^{-3}. Extinction effects were negligible. Refined atomic coordinates are given in Table 1, selected bond lengths and angles in Table 2.

Complete atomic coordinates, thermal parameters and bond lengths and angles have been deposited at the Cambridge Crystallographic Data Centre. See Instructions for Authors, *J. Chem. Soc., Dalton Trans.*, 1996, Issue 1.

NMR Measurements

Solutions of $[Mo_4Se_4(edta)_2]^{n-}$, n = 2–4, (8–16 mM), in 1.0 M $LiClO_4$, and of $[Mo_4S_4(H_2O)_{12}]^{5+}$ (17 mM) in 2.0 M $HClO_4$, each with added D_2O, were used. The ^{77}Se and ^{95}Mo NMR spectra were obtained at frequencies of 95.4 and 32.6 MHz respectively on a Bruker AMX500 spectrometer using 10 mm outside diameter spinning tubes. For both nuclei the spectral width was 100 kHz (corresponding to 1048 and 3067 ppm, respectively) and the chemical shifts are relative to external

Table 1 Atomic coordinates (× 10^4) for $Na_{2.5}H_{0.5}[Mo_4Se_4(edta)_2]\cdot 10H_2O$

Atom	*x*	*y*	*z*	Atom	*x*	*y*	*z*
Mo(1)	7 071.1(7)	7 730.9(9)	2 943.3(4)	C(14)	6 368(9)	10 595(10)	1 029(5)
Mo(2)	8 532.5(7)	8 043.5(9)	2 389.0(5)	O(9)	5 846(7)	11 015(8)	660(4)
Mo(3)	7 047.2(7)	9 281.3(9)	2 023.5(4)	O(10)	6 204(6)	9 712(7)	1 287(4)
Mo(4)	6 980.6(7)	7 005.1(9)	1 838.9(4)	C(15)	7 538(9)	11 712(11)	2 107(6)
Se(1)	7 908.4(9)	9 451.8(12)	2 955.9(6)	C(16)	6 668(8)	11 605(10)	2 328(5)
Se(2)	7 970.1(9)	6 240.0(11)	2 631.6(6)	O(11)	6 340(6)	12 408(7)	2 506(4)
Se(3)	7 910.8(10)	8 280.0(11)	1 396.6(6)	O(12)	6 340(5)	10 629(7)	2 307(4)
Se(4)	5 842.0(8)	8 087.8(10)	2 206.3(5)	C(17)	10 106(10)	9 423(13)	2 858(8)
N(1)	6 045(7)	5 587(8)	1 895(4)	C(18)	10 063(11)	8 453(13)	3 219(8)
C(1)	5 564(9)	5 426(11)	2 394(5)	O(13)	10 598(9)	8 359(12)	3 640(7)
C(2)	6 093(10)	5 293(11)	2 955(5)	O(14)	9 451(7)	7 772(8)	3 106(5)
N(2)	6 331(7)	6 320(8)	3 285(4)	C(19)	10 054(10)	8 974(13)	1 874(9)
C(3)	5 350(8)	5 746(11)	1 411(5)	C(20)	10 155(10)	7 727(13)	1 883(7)
C(4)	5 629(9)	6 309(11)	929(5)	O(15)	10 770(7)	7 299(9)	1 696(5)
O(1)	5 281(9)	6 081(9)	460(4)	O(16)	9 538(6)	7 173(8)	2 045(5)
O(2)	6 192(6)	7 062(7)	1 037(4)	Na(1)	5 000	10 000	0
C(5)	6 536(9)	4 557(10)	1 797(5)	Na(2)	5 271(4)	12 511(5)	167(2)
C(6)	7 194(9)	4 730(11)	1 427(6)	Na(3)	3 931(7)	4 892(7)	247(3)
O(3)	7 441(8)	3 931(8)	1 174(5)	O(20)	3 918(7)	11 461(8)	−93(4)
O(4)	7 502(6)	5 685(7)	1 379(4)	O(21)	5 391(7)	11 196(10)	−720(4)
C(7)	5 537(9)	6 827(11)	3 471(5)	O(22)	6 605(8)	13 378(10)	147(5)
C(8)	5 719(10)	7 967(12)	3 709(6)	O(23)	3 124(7)	5 448(9)	934(5)
O(5)	5 357(8)	8 304(8)	4 092(4)	O(24)	7 439(15)	6 029(17)	175(7)
O(6)	6 258(6)	8 533(7)	3 482(4)	O(25)	3 541(7)	7 562(9)	1 353(4)
C(9)	6 892(11)	5 913(12)	3 802(6)	O(26)	8 703(9)	4 891(15)	746(6)
C(10)	7 465(11)	6 808(12)	4 081(6)	O(27)	1 900(11)	8 626(14)	1 229(8)
O(7)	7 631(8)	6 759(10)	4 601(4)	O(28)	2 071(19)	8 044(24)	140(12)
O(8)	7 766(7)	7 499(8)	3 765(4)	O(29)	10 303(21)	5 864(27)	815(13)
N(3)	7 722(7)	10 793(8)	1 736(4)	O(30)	8 269(24)	4 734(32)	−251(15)
C(11)	8 660(9)	10 787(11)	1 680(7)	O(31)	8 518(32)	9 196(42)	4 381(20)
C(12)	9 289(10)	10 552(12)	2 182(8)	O(32)	10 553(35)	10 985(45)	997(22)
N(4)	9 556(7)	9 374(9)	2 309(6)	O(33)	9 336(31)	7 066(40)	5 185(19)
C(13)	7 250(10)	11 061(12)	1 162(6)				

Me_2Se and 2 M $Na_2[MoO_4]$. In each case a total shift range from −8000 to +8000 ppm was examined. For the paramagnetic samples the pulse-repetition interval was 0.010 s, and for the diamagnetic it was 0.30 s, and the total accumulation time per spectral region was *ca.* 2 h.

Magnetic studies

Magnetic susceptibility studies were made using a Quantum Design MPMS SQUID magnetometer with an applied field of 1 T. The powdered sample was contained in a calibrated gelatine capsule held in the centre of a soda straw fixed to the end of the sample rod. The magnetisation values of the instrument were calibrated against a standard palladium sample, supplied by Quantum Design, and also against chemical calibrants such as $CuSO_4\cdot 5H_2O$ and $[Ni(en)_3][S_2O_3]$ (en = ethane-1,2-diamine).

Infrared spectra

Spectra of KBr discs were recorded on a Nicolet 20PC FTIR instrument.

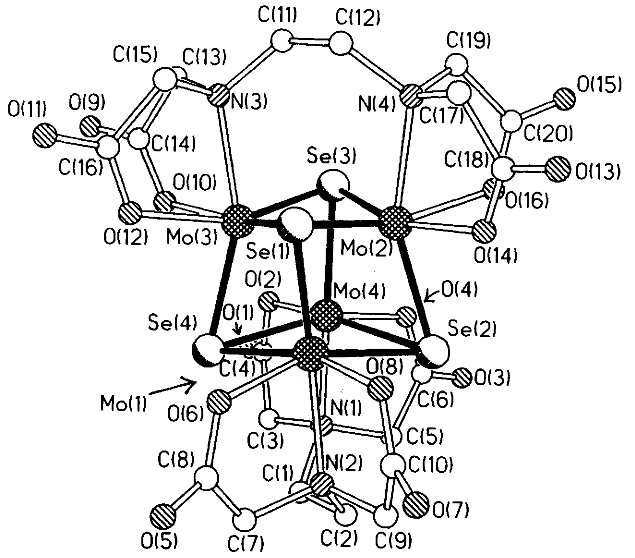

Fig. 2 Structure of the $[Mo_4Se_4(edta)_2]^{3-}$ anion without hydrogen atoms and including atom labels

Results

Crystal structure

The structure of $[Mo_4Se_4(edta)_2]^{3-}$ is shown in Fig. 2. Mean geometric parameters are: Mo···Mo 2.848, Mo–Se 2.479, Mo–O 2.156 and Mo–N 2.289 Å; Se–Mo–Se 106.6 and Mo–Se–Mo 70.1°. For each of these there is a range of values well in excess of individual parameter estimated standard deviations (e.s.d.s), but there is no clear pattern in the variations.

The formula applying to the crystalline sample is $Na_{2.5}H_{0.5}[Mo_4Se_4(edta)_2]\cdot 10H_2O$. Each sodium ion is approximately octahedrally co-ordinated by a mixture of aqua ligands and edta oxygen atoms, and these octahedra variously share faces and edges. The other water molecules of crystallisation are not co-ordinated. The well ordered ones form hydrogen bonds with edta and aqua ligands, while the disordered ones are located in channels and cavities in the structure.

NMR Studies

The ^{77}Se and ^{95}Mo NMR chemical shifts and linewidths observed, *e.g.* Figs. 3 and 4, are summarised in Table 3. Solutions of paramagnetic $[Mo_4Se_4(edta)_2]^{3-}$ were found to be stable for

Table 2 Selected bond lengths (Å) and angles (°)

Mo(1) ··· Mo(2)	2.827(2)	Mo(1) ··· Mo(3)	2.923(2)
Mo(1) ··· Mo(4)	2.810(2)	Mo(2) ··· Mo(3)	2.813(2)
Mo(2) ··· Mo(4)	2.901(2)	Mo(3) ··· Mo(4)	2.812(2)
Mo(1)–Se(1)	2.471(2)	Mo(1)–Se(2)	2.477(2)
Mo(1)–Se(4)	2.485(2)	Mo(2)–Se(1)	2.480(2)
Mo(2)–Se(2)	2.469(2)	Mo(2)–Se(3)	2.494(2)
Mo(3)–Se(1)	2.486(2)	Mo(3)–Se(3)	2.485(2)
Mo(3)–Se(4)	2.467(2)	Mo(4)–Se(2)	2.487(2)
Mo(4)–Se(3)	2.470(2)	Mo(4)–Se(4)	2.476(2)
Mo(1)–N(2)	2.290(10)	Mo(2)–N(4)	2.306(11)
Mo(3)–N(3)	2.278(10)	Mo(4)–N(1)	2.281(10)
Mo(1)–O(6)	2.173(9)	Mo(1)–O(8)	2.161(10)
Mo(2)–O(14)	2.130(10)	Mo(2)–O(16)	2.155(9)
Mo(3)–O(10)	2.142(9)	Mo(3)–O(12)	2.144(8)
Mo(4)–O(2)	2.164(9)	Mo(4)–O(4)	2.178(9)
Se(1)–Mo(1)–Se(2)	107.83(6)	Se(1)–Mo(1)–Se(4)	102.59(6)
Se(2)–Mo(1)–Se(4)	108.93(6)	Se(1)–Mo(2)–Se(2)	107.80(7)
Se(1)–Mo(2)–Se(3)	108.95(6)	Se(2)–Mo(2)–Se(3)	103.19(6)
Se(1)–Mo(3)–Se(3)	109.06(6)	Se(1)–Mo(3)–Se(4)	102.71(6)
Se(3)–Mo(3)–Se(4)	108.06(6)	Se(2)–Mo(4)–Se(3)	103.37(6)
Se(2)–Mo(4)–Se(4)	108.94(6)	Se(3)–Mo(4)–Se(4)	108.29(6)
Mo(1)–Se(1)–Mo(2)	69.62(6)	Mo(1)–Se(1)–Mo(3)	72.27(5)
Mo(2)–Se(1)–Mo(3)	69.01(5)	Mo(1)–Se(2)–Mo(2)	69.72(5)
Mo(1)–Se(2)–Mo(4)	68.96(5)	Mo(2)–Se(2)–Mo(4)	71.68(5)
Mo(2)–Se(3)–Mo(3)	68.81(5)	Mo(2)–Se(3)–Mo(4)	71.54(6)
Mo(3)–Se(3)–Mo(4)	69.14(5)	Mo(1)–Se(4)–Mo(3)	72.35(5)
Mo(1)–Se(4)–Mo(4)	69.01(5)	Mo(3)–Se(4)–Mo(4)	69.34(5)

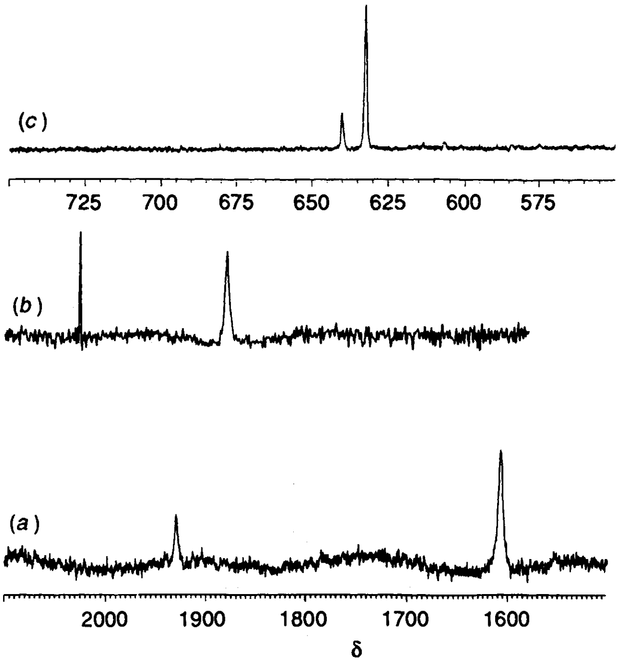

Fig. 3 The ^{77}Se NMR spectra measured at 95.5 MHz for (*a*) $[Mo_4Se_4(edta)_2]^{3-}$, (*b*) $[Mo_4Se_4(edta)_2]^{2-}$ and (*c*) $[Mo_4Se_4(edta)_2]^{4-}$ (note different scale)

extended periods of time and virtually unchanged spectra were obtained after an interval of several weeks. The ^{77}Se signals sharpened somewhat at higher temperatures. That at δ 1607 showed a temperature coefficient of −1.0 ppm per °C, and that at δ 1931 had a temperature coefficient of −2.8 ppm per °C, both presumably attributable to the paramagnetism. Samples appeared to contain small amounts of $[MoO_4]^{2-}$ as evidenced by a sharp Mo signal ($\nu_{\frac{1}{2}} \approx 10$ Hz) at δ −1.0.

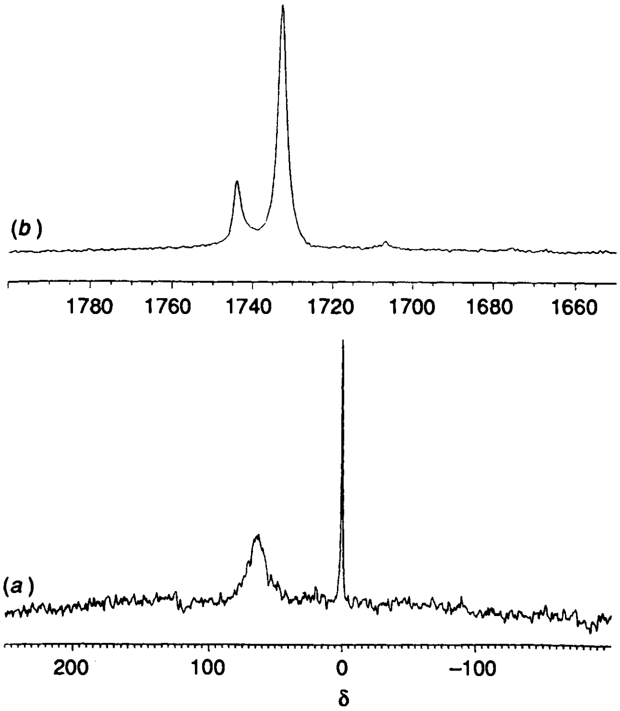

Fig 4 The ^{95}Mo NMR spectra measured at 32.6 MHz for (*a*) $[Mo_4Se_4(edta)_2]^{3-}$ (the sharp signal at δ 0.0 is due to $[MoO_4]^{2-}$) and (*b*) $[Mo_4Se_4(edta)_2]^{4-}$ (note different scale)

Solutions of $[Mo_4Se_4(edta)_2]^{2-}$ were much less stable, even with rigorous exclusion of air, and were stored frozen prior to measurement at 3 °C. They were always paramagnetic, possibly owing to contamination by unoxidised $[Mo_4Se_4(edta)_2]^{3-}$. Although Fig. 3(*b*) is included as a matter of record, it is not appropriate to discuss the ^{77}Se NMR spectrum of $[Mo_4Se_4(edta)_2]^{2-}$ in detail at this stage. At 25 °C the ^{77}Se signal at δ 1880 was much broader, but regained its original width on recooling to 3 °C. After storage for 2 weeks at 25 °C both ^{77}Se signals had disappeared and there was evidence for the formation of $[Mo_4Se_4(edta)_2]^{3-}$. For technical reasons it was not possible to obtain a ^{95}Mo NMR spectrum at 3 °C, and the reported signal obtained at 25 °C after 15 h of storage at that temperature may arise from $[Mo_4Se_4(edta)_2]^{3-}$. There was also evidence for $[MoO_4]^{2-}$ in this spectrum.

Solutions of $[Mo_4Se_4(edta)_2]^{4-}$ were stable for several days provided that air was completely excluded. In all cases confirmation of the diamagnetic/paramagnetic nature of the solutions was provided by the sharpness of the deuterium lock signal.

Magnetic properties

The crystalline sample of $[Mo_4S_4(H_2O)_{12}][pts]_5 \cdot 14H_2O$ showed Curie-like behaviour with corresponding μ values independent of temperature. The moment remains constant at 1.78 μ_B between 300 and 20 K and then decreases a little towards 1.73 μ_B at 4.2 K. Fitting of the χ^{-1} *versus* temperature data shown in Fig. 5 by the Curie–Weiss equation $\chi = C(T - \theta)^{-1}$ yielded best-fit values of $C = 0.395$ emu K, $\theta = -0.19$ K for χ (diamagnetism) = -799×10^{-6} emu. These compare reasonably well to the values deduced for $Na_3[Mo_4S_4(edta)_2] \cdot 10H_2O$ by Sugano *et al.*:[7] $C = 0.525$ emu K, $\theta = -2.0$ K, χ (diamagnetism) = -300×10^{-6} emu. The *C* value in the case of the edta complex is larger than anticipated and has been related[7] to the large observed values of $\bar{g}$, *viz.* 2.32 or 2.48.[1,5]

The bulk susceptibility data indicate that thermal population of an $S = \frac{1}{2}$ ground state occurs at all temperatures, and the state must be isolated energetically since there is no evidence of any other level being populated at higher temperatures. This contrasts with the susceptibility data on mixed-valence $[Fe_4S_4(SR)_4]^{3-}$ clusters which, even in $S = \frac{1}{2}$ ground state, show the population of higher spin states at temperatures above *ca.* 30 K, leading to significantly higher μ values than 1.73 μ_B.[12,13]

Table 3 Summary of NMR chemical shifts, linewidths and relative intensities (r.i.) for the different clusters studied

Cluster	δ	^{77}Se $\nu_{\frac{1}{2}}$/Hz	r.i.	δ	^{95}Mo $\nu_{\frac{1}{2}}$/Hz	r.i.	*T*/°C
$[Mo_4Se_4(edta)_2]^{3-}$	+1607(3)	550	1.0(2)	+62(3)	300	—	22
	+1931(4)	380	0.4(1)				
$[Mo_4Se_4(edta)_2]^{2-}$	+1880(6)	1200	1.0(2)				
	+2028(10)	100	0.35(1)	+54(3)	300	—	3
$[Mo_4Se_4(edta)_2]^{4-}$	+634(1)	7	1.0(2)	+1733(3)	80	1.0(2)	22
	+641(1)	7	0.3(1)	+1744(3)	60	0.25(1)	
$[Mo_4S_4(edta)_2]^{3-}$				+5889(10)	500	1.0(2)	22
				−3331(12)	500	0.5(1)	
				−3399(15)	500	0.25(10)	
$[Mo_4S_4(H_2O)_{12}]^{5+}$				+5880(10)	500	—	22

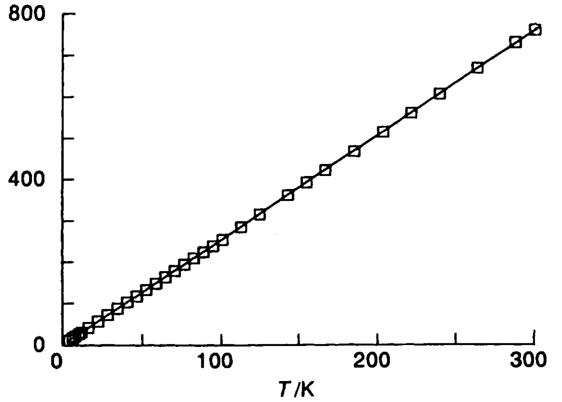

Fig. 5 Plot of χ^{-1} (per mol) *versus* temperature for $[Mo_4S_4(H_2O)_{12}]$-$[pts]_5 \cdot 14H_2O$. The solid line is that calculated using a Curie–Weiss law, $\chi = C(T - \theta)^{-1}$, with values of C and θ given in the text

The susceptibility data for the $[Mo_4S_4(H_2O)_{12}][pts]_5 \cdot 14H_2O$ complex are generally compatible with the results of the 3.8–100 K EPR spectroscopic study made on a frozen aqueous solution sample.[1] The temperature-independent EPR spectrum gave a $\bar{g}$ value of 2.25 from which μ_{calc} is 1.95 μ_B, higher than the value observed here. Changing the quantisation of the principal g values from those given[1] yields $\bar{g}$ = 2.03 and a moment of 1.75 μ_B, as observed.

Infrared studies

The spectrum of a sample of $[Mo_4S_4(H_2O)_{12}]Cl_5$ in the region 800–300 cm^{-1} is shown in Fig. 6. Comparisons are made with $[Mo_3S_4(H_2O)_9]Cl_4$. Intense bands due to H_2O absorption at 3600–3200 (antisymmetric and symmetric OH stretch) and at 1600 cm^{-1} (HOH bonding) were observed in both cases. Other wide bands at around 600 cm^{-1} may also be due to co-ordinated H_2O (librational modes).[14] The band at 459 cm^{-1} for $[Mo_4S_4(H_2O)_{12}]^{5+}$ {461 cm^{-1} for $[Mo_3S_4(H_2O)_9]^{4+}$} is assigned to Mo–μ_3-S vibrations. The experimental and calculated vibrational frequencies of such Mo–μ_3-S bonds have been reported for the isotopically labelled $[Mo_3S_7Y_6]^{2-}$ clusters ($Y^- = Cl^-$ or Br^-).[15] A corresponding band is present also at 433 and/or 448 cm^{-1} for $[Mo_4S_4(CN)_{12}]^{8-}$,[16] and this frequency is one of the best characterised in the IR and Raman spectra of these clusters. An intense band at 355 cm^{-1} for $[Mo_3S_4(H_2O)_9]^{4+}$ may belong to vibrations involving μ-S atoms. In the case of $[Mo_3S_7Cl_6]^{2-}$ such Mo–μ-S frequencies fall in the 330–390 cm^{-1} region,[15] but are strongly mixed with Mo–Cl bands. There is another strong band at 494 and shoulder at ≈440 cm^{-1} for $[Mo_3S_4(H_2O)_9]^{4+}$. The $[Mo_4S_4(H_2O)_{12}]^{5+}$ cluster gives bands at 338mw and 351 (sh) cm^{-1}, and weaker absorptions at 420 and 400 cm^{-1}, which in some part relate to Mo–O stretching frequencies, Fig. 6. Details of these spectra in the context of the present work suggest that an extension of these studies to include isotope labelling would be worthwhile.

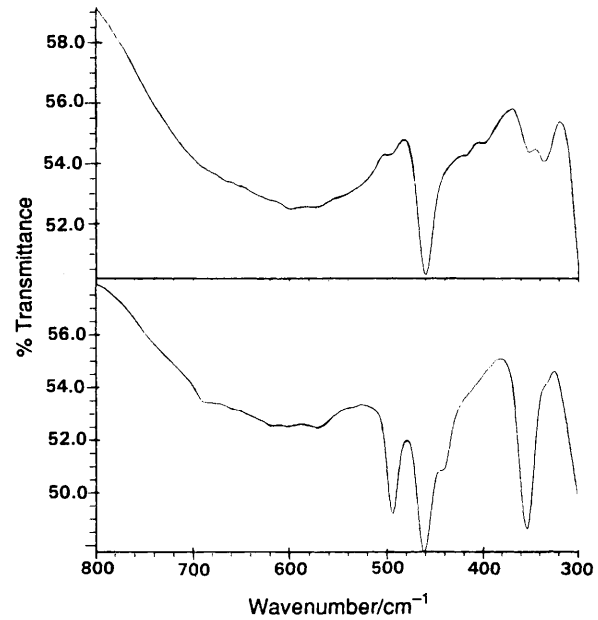

Fig. 6 Fourier-transform infrared spectra of the mixed-valence (3.25) cuboidal cluster $[Mo_4S_4(H_2O)_{12}]Cl_5$ (solid) in a KBr disc (upper), and (for comparison) the corresponding trinuclear incomplete-cuboidal $Mo^{IV}{}_3$ cluster $[Mo_3S_4(H_2O)_9]Cl_4$ (lower)

Discussion

The geometry of the Mo_4Se_4 core is essentially identical to that of the $[Mo_4Se_4(H_2O)_{12}]^{5+}$ cation, in the hydrated toluene-*p*-sulfonate salt,[4] and the replacement of aqua by edta ligands does not significantly affect the structure. The same conclusion is drawn from a comparison of corresponding sulfido-bridged clusters, specifically the $[Mo_4S_4(H_2O)_{12}]^{5+}$ cation and the $[Mo_4S_4(edta)_2]^{3-}$ anion,[17] but changing the overall charge on the core does produce significant changes in the geometry, especially in Mo ··· Mo distances, as evidenced by the series $[Mo_4S_4(edta)_2]^{n-}$, with n = 2–4.[17] The observed differences in the geometry of the $[Mo_4S_4(edta)_2]^{3-}$ and $[Mo_4Se_4(edta)_2]^{3-}$ ions can be ascribed to the difference in size of the bridging sulfido and selenido atoms which leads to Mo ··· Mo distances *ca.* 0.04 Å longer.

In assessing the NMR spectra of the $[Mo_4Se_4(edta)_2]^{n-}$ anions it is important to appreciate that whilst the line broadening in the case of ^{77}Se can arise from the effects of paramagnetism alone, the ^{95}Mo signals will also be broadened by quadrupolar relaxation ($I = \frac{5}{2}$), and some may not be observable at all. Thus an absence of peak correlations between the spectra of the two nuclei may not be significant.

From the widths of the ^{77}Se resonances and the appearance of the deuterium lock signal it seems that the solutions of $[Mo_4Se_4(edta)_2]^{2-}$ are paramagnetic. This could arise from paramagnetism of the cluster itself or from the presence of residual unoxidised $[Mo_4Se_4(edta)_2]^{3-}$ in the unstable sample. In the solid state $[Mo_4S_4(edta)_2]^{2-}$ has been found[7] to be diamagnetic which would favour the second interpretation. This diamagnetism has been ascribed to the metal HOMO (highest occupied molecular orbital) as being a_1 rather than t_2 so that the two degenerate e and the three degenerate t_2 orbitals are filled by the ten excess electrons, which are therefore all paired. However, it is recognised that in these cubane analogues with from eight to eleven excess electrons small deviations from T_d symmetry can affect the splitting and energies of the orbitals and hence lead to complex magnetic behaviour. For example, $[Mo_4S_4(S_2CNEt_2)_6]$ (ten excess electrons) is paramagnetic which is consistent with either the t_2 or e orbitals being of highest energy.[18] Similar considerations may well apply to $[Mo_4Se_4(edta)_2]^{2-}$ which could therefore also be inherently paramagnetic with a magnetic moment corresponding to $S = 1$. We plan to carry out further magnetic measurements on this species.

Two different explanations can be put forward to account for the NMR results. First of all the observation that for solutions of $[Mo_4Se_4(edta)_2]^{3-}$ there are two separate ^{77}Se signals in an intensity ratio of 2.5 ± 0.5:1 provides evidence for valence trapping of $Mo^{III}{}_3Mo^{IV}$, with the lower-intensity signal arising from the ^{77}Se on the vertex of the cube opposite to the Mo^{IV}. The failure to detect two corresponding ^{95}Mo signals can be attributed to excessive broadening of one signal as a consequence of the quadrupole moment, and/or greater unpaired spin density on Mo^{III} (d^3) than on Mo^{IV} (d^2). The observation of separate ^{77}Se signals with a frequency separation of *ca.* 31 000 Hz implies that the valence-trapped species has a lifetime in excess of 2×10^{-5} s. However, doubt is cast upon this interpretation by the results for the reduced cube $[Mo_4Se_4(edta)_2]^{4-}$ in which irrespective of valence trapping the state will be $Mo^{III}{}_4$ so that a single selenium line would result. In the oxidised $[Mo_4Se_4(edta)_2]^{2-}$ cube valence trapping would give a $(Mo^{IV}Mo^{III})_2$ state with an expected pair of ^{77}Se signals in a 1 : 1 intensity ratio. In fact, all three solutions have *two* ^{77}Se signals with roughly the same intensity ratio of *ca.* 3:1 which strongly suggests the presence of two different independent species in each case.

In the second explanation we suggest that both solutions contain essentially the same Mo_4Se_4 core, with average molybdenum oxidation states of 3.25, 3.5 and 3.0 in $[Mo_4Se_4(edta)_2]^{3-}$, $[Mo_4Se_4(edta)_2]^{2-}$ and $[Mo_4Se_4(edta)_2]^{4-}$, respectively. The observation of two ^{77}Se signals in each case would then arise from the presence of two forms, which differ in the manner/extent of co-ordination of the Mo by edta and possibly H_2O. In the case of diamagnetic $[Mo_4Se_4(edta)_2]^{4-}$ the difference in co-ordination has only a small effect upon chemical shifts, as would be expected, but in paramagnetic $[Mo_4Se_4(edta)_2]^{3-}$ and possibly also $[Mo_4Se_4(edta)_2]^{2-}$ the effects are apparently more substantial. Comparatively small variations in the co-ordination of Mo could lead to changes in either the Fermi contact[19] or the isotropic pseudo-contact[20] interactions at Se, which would produce sizeable paramagnetic shifts in the directions observed. The sign of the temperature dependence of the ^{77}Se shifts for $[Mo_4Se_4(edta)_2]^{3-}$ is consistent with this interpretation, as is the fact that the more shifted resonance (at δ 1931) has the larger temperature coefficient.

For the more stable paramagnetic sulfur analogue $[Mo_4S_4(edta)_2]^{3-}$ three ^{95}Mo signals were recorded, and one of these is at a position very close to that from $[Mo_4S_4(H_2O)_{12}]^{5+}$ in which no edta is present, whereas the others are substantially shifted. This also supports the idea that variations in the ligands surrounding the Mo can lead to large changes in the paramagnetic shifts.

Overall we conclude that whilst the ^{77}Se NMR spectrum of $[Mo_4Se_4(edta)_2]^{3-}$ is consistent with the presence in solution of valence-trapped species with lifetimes in excess of 10^{-5} s, this is not supported by the spectra of the other complexes. It appears more likely that the multiple NMR signals arise from the presence *in solution* of species which differ only slightly in the mode of co-ordination of edta, or the extent of co-ordination by H_2O and edta in the overall structure. The crystal structure was obtained for a form which crystallises preferentially.

Molecular models indicate that the CH_2–CH_2 bonds of the co-ordinated edta molecules can adopt two possible conformations, in which they are approximately parallel to one or the other pair of edges of the adjacent face of the Mo_4Se_4 cube. There are thus two isomers of the complex possible in which the CH_2–CH_2 bonds of the two edta moieties are mutually either approximately parallel giving a complex with D_2 symmetry, or approximately perpendicular giving a complex with S_4 symmetry. In the solid the former situation applies, presumably owing to crystal-packing forces, but in solution both forms are to be expected. However, it seems unlikely that this can account for our NMR observations because the two forms will be of very similar energy and should be present in equal proportions, and the barrier to their interconversion by a conformational flip of the edta is expected to be low.

Whilst it is unlikely that the solvent water molecules will be able to displace ligating atoms of the edta, it is known that Mo^{III} and Mo^{IV} can have higher co-ordination numbers as in $[Mo(CN)_7]^{4-}$ and $[Mo(CN)_8]^{4-}$.[21,22] Also, high-spin d^5 edta complexes of Mn^{II} and Fe^{III} have been shown by X-ray crystallography to have seven-co-ordinate $[Mn(edta)(H_2O)]^{2-}$ and $[Fe(edta)(H_2O)]^{-}$ structures.[23,24] Thus the additional species present in solution may involve further co-ordination of H_2O at Mo. This tendency is thought to be enhanced by the angular strain that can be induced by hexadentate edta, although it must be pointed out that in the structure of $[Mo_4Se_4(edta)_2]^{3-}$ (and probably the other complexes also) the constraints of the tetradentate edta and the cube would not appear to favour seven-co-ordination. Finally, it must be stressed that our NMR observations do not preclude the possibility of valence-trapped species with lifetimes shorter than 10^{-6} s.

The magnetic study on crystalline $[Mo_4S_4(H_2O)_{12}][pts]_5 \cdot 14H_2O$ was undertaken primarily to determine the spin of the ground state but also to attempt to shed light on trapped-*versus* average-valence states on the molybdenum centres of the cube. Such knowledge in $[Fe_4E_4]^{n+}$ (E = S or Se) mixed-valence cubane systems has advanced rapidly in recent years through a combination of experimental and theoretical studies and the effects of Heisenberg exchange and double-exchange coupling (from delocalised electrons) have been delineated.[12,13,25,26] The magnetic properties of $[Mo_4E_4]^{n+}$ cubes are less well understood and are potentially complicated by metal–metal bonding effects which make molecular orbital models perhaps more relevant than Heisenberg spin-coupling models.[7,17] In order to achieve an isolated $S = \frac{1}{2}$ state in the present case a distortion of the cube (*e.g.* D_{2d} symmetry) would need to be involved such that the eleven metal-based bonding electrons would occupy the Mo ··· Mo bonding orbitals leading to the HOMO level being e^1 (derived from the t_2 level in T_d symmetry). This splitting of the t_2 level has been proposed[5,8,17,27] for $[Mo_4S_4(edta)_2]^{3-}$ and, together with the local symmetry generated by the terminal ligands, is presumably responsible for the anisotropy in the EPR *g* values. The origin of the t_2 splitting is not clear but may involve Jahn–Teller as well as structural distortions, the latter being small in size for the aqua and edta cubes.[17] Shibahara *et al.*[17] have recently come to somewhat similar conclusions and have also included spin-polarisation effects in molecular orbital calculations, carried out in both T_d and D_{2d} symmetry. Perusal of the electronic levels in Fig. 6 of ref. 17 suggests an e–b_2 splitting in D_{2d} symmetry (from t_2) of *ca.* 250 cm^{-1} and a t_2–e separation (assuming T_d symmetry) of *ca.* 6500 cm^{-1} for

$[Mo_4S_4(H_2O)_{12}]^{5+}$. The present magnetic data and the EPR data[1] are generally compatible with such energies.

The alternative use of Heisenberg spin-coupling models to explain the present variable-temperature magnetic data would require very large negative J values. Interestingly, the dinuclear mixed-valent complex $[(tacn)Mo^{III}(\mu\text{-}O)(\mu\text{-}O_2CMe)_2Mo^{IV}(tacn)][PF_6]_3$, where tacn is 1,4,7-triazacyclononanane, and the Mo–Mo bond length of 1.97 Å also shows an $S = \frac{1}{2}$ ground state,[28] but displays a small increase in the magnetic moment values at temperatures above 100 K on account of population of accessible $S = \frac{3}{2}$ levels, J in this case being -150 cm^{-1} and $g = 1.89$. A molecular-orbital model having a Mo–Mo antibonding HOMO of symmetry $\pi(a_1)^1$, in C_{2v} symmetry, was simultaneously used to rationalise the $S = \frac{1}{2}$ ground state. Implicit in this MO treatment, and that of a similarly behaved $Ru^{III/IV}$ dimer,[7] is the assumption of a non-trapped valency on the metal centre with average oxidation state $M^{3.5+}$.

In summary, the magnetic and EPR data for the present μ-sulfido aqua complex and the edta analogue clearly show an $S = \frac{1}{2}$ ground state at all temperatures.[5,7,17] It is not possible definitively to assign the trapped $Mo_3{}^{III}Mo^{IV}$ valencies *versus* the delocalised $Mo^{3.25+}$ state from either the structural or magnetic data, and thus the initial postulate of $Mo^{3.25+}$ (Class III delocalised) remains tenable.[1,5]

Infrared studies on the mixed-valence $[Mo_4S_4(H_2O)_{12}]^{5+}$ cluster indicate the potential of this method to provide further evidence for a localised albeit short-lived $Mo_3{}^{III}Mo^{IV}$ structure. Time constraints in vibrational spectroscopy at $\approx 10^{-11}$ s are not likely to be a problem in detecting localised structures. From the NMR studies described it is concluded that the lifetime of an $Mo_3{}^{III}Mo^{IV}$ state is $< 10^{-6}$ s. Rate constants for the formation/decay of ion pairs are close to 10^9 s^{-1},[28–30] and a value of this magnitude is believed to hold in the case of $[Mo_4S_4(H_2O)_{12}]^{5+}$, NCS^- which is formed prior to NCS^- for H_2O substitution on $[Mo_4S_4(H_2O)_{12}]^{5+}$.

We conclude therefore that the lifetime of a localised $Mo_3{}^{III}Mo^{IV}$ state is likely to be between 10^{-6} and 10^{-9} s.

Acknowledgements

We are grateful to the University of Newcastle (D. M. S.) and the UK Science and Engineering Research Council now EPSRC (A. G. S. and W. C.) for financial support, and the Leverhulme Trust for a Fellowship to (W. McF.). Grants from the Australian Research Council (to K. S. M. and B. M.) are also gratefully acknowledged.

References

1 Y.-J. Li, M. Nasreldin, M. Humanes and A. G. Sykes, *Inorg. Chem.*, 1992, **31**, 3011.
2 B.-L. Ooi and A. G. Sykes, *Inorg. Chem.*, 1989, **28**, 3799.
3 D. T. Richens, P.-A. Pittet, A. E. Merbach, M. Humanes, G. J. Lamprecht, B.-L. Ooi and A. G. Sykes, *J. Chem. Soc., Dalton Trans.*, 1993, 2305.
4 M. Nasreldin, G. Henkel, G. Kampmann, B. Krebs, G. J. Lamprecht, C. A. Routledge and A. G. Sykes, *J. Chem. Soc., Dalton Trans.*, 1993, 737.
5 T. Shibahara, H. Kuroya, K. Matsumoto and S. Ooi, *J. Am. Chem. Soc.*, 1984, **106**, 789.
6 H. Akashi, T. Shibahara, T. Narahara, H. Tsura and H. Kuroya, *Chem. Lett.*, 1989, 129.
7 T. Sugano, T. Shibahara, H. Kobayashi, N. Uryu and M. Kinoshita, *Bull. Chem. Soc. Jpn.*, 1988, **61**, 1785.
8 P. W. Dimmock, J. McGinnis, B.-L. Ooi and A. G. Sykes, *Inorg. Chem.*, 1990, **29**, 1085.
9 J. Cosier and A. M. Glazer, *J. Appl. Crystallogr.*, 1986, **19**, 105.
10 W. Clegg, *Acta Crystallogr., Sect. A*, 1981, **37**, 22.
11 G. M. Sheldrick, *SHELXTL users manual*, Siemens Analytical X-Ray Instruments Inc., Madison, WI, 1994; G. M. Sheldrick, SHELXL 93, program for crystal structure refinement, University of Göttingen, 1993.
12 M. J. Carney, G. C. Papaefthymiou, K. Spartalian, R. B. Frankel and R. H. Holm, *J. Am. Chem. Soc.*, 1988, **110**, 6084.
13 K. S. Murray, *Adv. Inorg. Chem.*, 1995, **43**, 261.
14 K. Nakamoto, *Infrared and Raman Spectra of Inorganic and Coordination Compounds*, 4th edn., Wiley, New York, 1986, p. 229.
15 V. P. Fedin, M. N. Sokolov, Y. V. Mironov, B. A. Kolesov, S. W. Tkachev and V. E. Fedorov, *Inorg. Chim. Acta*, 1990, **167**, 39.
16 A. Müller, R. Jostes, W. Eltzner, C.-S. Nie, E. Dieman, H. Bögge, M. Zimmermann, M. Dartmann, U. Reinsch-Vogell, S. Che, S. J. Cyvin and B. N. Cyvin, *Inorg. Chem.*, 1985, **24**, 2872.
17 T. Shibahara, H. Kuroya, H. Akashi, K. Matsumoto and S. Ooi, *Inorg. Chim. Acta*, 1993, **212**, 251.
18 T. C. W. Mak, K. S. Jasim and C. Chieh, *Inorg. Chem.*, 1985, **24**, 1587.
19 H. M. McConnell and D. B. Chesnut, *J. Chem. Phys.*, 1958, **28**, 107.
20 H. M. McConnell and R. E. Robertson, *J. Chem. Phys.*, 1958, **29**, 1361.
21 G. R. Rossman, F.-D. Tsay and H. B. Gray, *Inorg. Chem.*, 1973, **12**, 824.
22 S. S. Basson, J. G. Leipoldt, L. D. C. Bok, J. S. van Vollenhoven and P. J. Cilliers, *Acta Crystallogr., Sect. B*, 1980, **36**, 1765; J. G. Leipoldt, S. S. Basson and A. Roodt, *Adv. Inorg. Chem.*, 1993, **40**, 245.
23 S. Richards, B. Pedersen, J. V. Silverton and J. L. Hoard, *Inorg. Chem.*, 1964, **3**, 27.
24 M. D. Lind, M. J. Hamor, T. A. Hamor and J. L. Hoard, *Inorg. Chem.*, 1964, **3**, 34.
25 L. Noodleman and D. A. Case, *Adv. Inorg. Chem.*, 1992, **38**, 423.
26 M. Belinskii, *J. Chem. Phys.*, 1993, **172**, 189, 212; **173**, 27; **176**, 15, 37.
27 F. A. Cotton, M. P. Diebold, Z. Dori, R. Llusar and W. Schwetzer, *J. Am. Chem. Soc.*, 1985, **197**, 6735.
28 K. Wieghardt, U. Bossek, A. Neves, B. Nuber and J. Weiss, *Inorg. Chem.*, 1989, **28**, 432.
29 P. Neubold, K. Wieghardt, B. Nuber and J. Weiss, *Inorg. Chem.*, 1989, **28**, 459.
30 M. Eigen, W. Kruse and K. Tamm, *Z. Elektrochem.*, 1953, **57**, 103.

Received 22nd August 1995; *Paper* 5/05582B